

Nonlinear finite element analysis of top- and seat-angle with double web-angle connections

N. Kishi[†], A. Ahmed[‡] and N. Yabuki^{‡†}

Department of Civil Engineering, Muroran Institute of Technology, Muroran 050-8585, Japan

W.F. Chen^{‡‡}

College of Engineering, University of Hawaii, Manoa, Honolulu, HI 96822, U.S.A.

Abstract. Four finite element (FE) models are examined to find the one that best estimates moment-rotation characteristics of top- and seat-angle with double web-angle connections. To efficiently simulate the real behavior of connections, finite element analyses are performed with following considerations: 1) all components of connection (beam, column, angles and bolts) are discretized by eight-node solid elements; 2) shapes of bolt shank, head, and nut are precisely taken into account in modeling; and 3) contact surface algorithm is applied as boundary condition. To improve accuracy in predicting moment-rotation behavior of a connection, bolt pretension is introduced before the corresponding connection moment being surcharged. The experimental results are used to investigate the applicability of FE method and to check the performance of three-parameter power model by making comparison among their moment-rotation behaviors and by assessment of deformation and stress distribution patterns at the final stage of loading. This research exposes two important features: (1) the FE method has tremendous potential for connection modeling for both monotonic and cyclic loading; and (2) the power model is able to predict moment-rotation characteristics of semi-rigid connections with acceptable accuracy.

Key words: semi-rigid connection; moment-rotation behavior; connection stiffness and strength; monotonic loading; finite element method.

1. Introduction

In the ASD specification (1989), AISC categorizes steel beam-to-column connections into *Type I*, *II* and *III*. For *Type I*, it is assumed that beam-to-column connections have sufficient rigidity to hold the original angles virtually unchanged between intersecting members. For *Type II*, it is assumed that, insofar as gravity loading is concerned, ends of beams are connected for shear force only and are free to rotate under gravity load. For *Type III*, it is assumed that the connections of beams possess a dependable and known moment capacity intermediate in degree between the rigidity of *Type I* and the flexibility of *Type II*. In introducing LRFD specification (1994), AISC recategorized these into two groups: FR (fully restrained) connection (*Type I* of ASD) and PR (partially restrained)

[†] Professor

[‡] Graduate Student

^{‡†} Associate Professor

^{‡‡} Dean

connection (*Types II and III of ASD*). With reference to practical application of semi-rigid frame construction, this regrouping added little new. Moreover, despite recognition of PR i.e. semi-rigid connection, the new specifications did not provide design guidelines for the PR construction. This is largely because of a lack of consensus on what model is appropriate for representing moment-rotation behavior of semi-rigid connections, and of inadequate information to capture the different aspects of connection flexibility.

The aforementioned discussion reflects a need for greater understanding of the semi-rigid behavior of connections. This study addresses bolted top- and seat-angle with double web-angle connection, for several reasons. (1) Such connection typifies semi-rigid connection. (2) There is little ambiguity about it belonging to either of the other classifications (rigid-semi-rigid or semi-rigid-flexible). (3) It is easy to fabricate and does not require expensive field welding. (4) It has sufficient ductility and energy absorption capacity to resist earthquake forces and can be used as a semi-rigid connection in aseismic design.

Several experimental studies have addressed prediction of moment-rotation characteristics of top- and seat-angle with double web-angle connections (Rathbun 1936 and Azizinamini *et al.* 1985). These experimental works have been used to examine the validity of analytical studies. In the recent analytical studies, simple mathematical expressions were developed linking connection details to the moment-rotation curves using a method of curve-fitting the experimental data (e.g., Frye and Morris 1975, Kishi and Chen 1990 etc.). Rathbun (1936), Monforton and Wu (1963), and Lightfoot and LeMessurier (1974) proposed linear $M-\theta$ models in which initial connection stiffness is used as a key parameter. The accuracy of these models is limited and they are suitable for only a small range of initial relative rotation. Bilinear model (Tarpy and Cardinal 1981, Lui and Chen 1983) and piecewise linear model (Jones *et al.* 1980, 1981), despite some shortcomings, achieved a better approximation of the real connection behavior. Frye and Morris (1975) proposed the polynomial model to predict $M-\theta$ curve for several types of connections. However, this model inherently tends to produce negative stiffness in some cases, which seems physically impossible. Exponential model (Lui and Chen 1986), modified exponential model (Kishi and Chen 1986) and other exponential models (Yee and Melchers 1986, Wu and Chen 1990) were proposed independently to evaluate $M-\theta$ curve of connections. Models using power function, called power models (Colson and Louveau 1983, Kishi and Chen 1990), also have been reported. Use of the aforementioned prediction models is limited to monotonic loading. There is hardly any model that is available for cyclic loading. With the background of seismic loading problems, a finite element technique can be a good alternative approach to pursue the problem.

This study aims to develop an appropriate finite element methodology for efficiently predicting the behavior of top- and seat-angle with double web-angle connections. Validity of the finite element method is examined by comparing the calculation results of FE analysis with experimental results, with reference to the stress distribution in the angles and spread of yield zones at different stages of loading. This study further investigates the applicability of the power model developed by Kishi and Chen (1990) by making comparison among the moment-rotation curves of FE analysis, experimental results and three-parameter power model.

2. Top- and seat-angle with double web-angle connection

This type of connection is composed of four angles to connect a beam to a column. Among those,

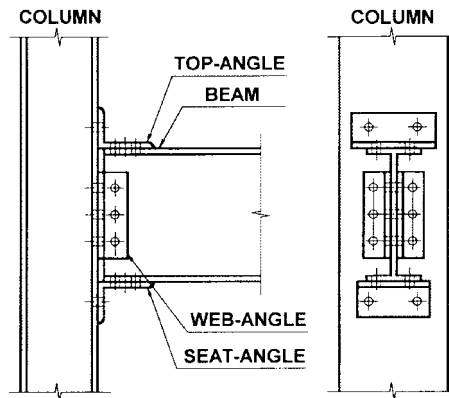


Fig. 1 Typical top- and seat-angle with double web-angle connection

two are web angles bolted to beam web and column flange and the others are top and seat angles located above and below the beam flanges and bolted to the beam and column flanges. A typical connection is shown in Fig. 1. The geometrical properties used in the analysis are taken from test data of Azizinamini *et al.* (1985), and are shown in Table 1.

3. Finite element model selection

Four three-dimensional (3D) FE models were setup under the ABAQUS (1998) standards for selection of the model that most closely reproduces the actual connection behavior. The connection is modeled using eight-node linear brick elements. It was chosen because a C3D8 element with full integration (eight Gauss points) is precise in the constitutive law integration and is suitable for plasticity problems. This type of element is appropriate for finite strain and rotation in large displacement analysis. The notations used to identify the four FE models are ND, NF, BM and BI. The character N denotes non-existence of bolts (i.e. bolts are not considered in the model); D denotes defined gage ($g-w/2$), F denotes full gage g , where g is the gage distance from the bolt hole centerline to the angle heel; and w is the width of bolt head. The character B indicates the presence of bolts in the mesh. M stands for monolithic and is used to mean that the bolts are monolithically jointed to the part of angle, column or beam flanges and beam web. I means independence, i.e. bolts act as independent components in the model. In formation of mesh geometry of FE models, connection geometry of the 14S2 test connection is strictly followed (Table 1). In brief, the four models can be described as follows.

Model ND- This model is shown in Fig. 2a. Bolts are not considered in constructing the mesh of the model. Angles are used to connect beam to column. All angle legs are viewed as being composed of two parts: i) the outer part from heel side (monolithically jointed to the column flange and beam flange or beam web); and ii) the inner part from heel side (considered to be free from column flange and beam flange or web). Contact model definition is applied in the free parts of angle legs. Contact areas for the flange and web angles free parts are rectangular consisting of angle length and gage distance ($g-w/2$).

Model NF- This model is the same as model ND, except the length of inner heel side parts of angle legs. In this case, the contact areas for the flange and web angles free parts are also

Table 1 Geometrical properties of connections used in analysis

Test ID	Beam section	Flange angles			Web angles		
		Angle section	Length (in)	Gage on column flange (in)	Bolt spacing on column flange (in)	Angle section	Length (in)
With $3/4$ in bolt diameter							
14S1	W14 × 38	$6 \times 4 \times 3/8$	8	$2 1/2$	$5 1/2$	$4 \times 3 1/2 \times 1/4$	$8 1/2$
14S2	W14 × 38	$6 \times 4 \times 1/2$	8	$2 1/2$	$5 1/2$	$4 \times 3 1/2 \times 1/4$	$8 1/2$
14S3	W14 × 38	$6 \times 4 \times 3/8$	8	$2 1/2$	$5 1/2$	$4 \times 3 1/2 \times 1/4$	$5 1/2$
14S4	W14 × 38	$6 \times 4 \times 3/8$	8	$2 1/2$	$5 1/2$	$4 \times 3 1/2 \times 3/8$	$8 1/2$
8S1	W8 × 21	$6 \times 3 1/2 \times 5/16$	6	2	$3 1/2$	$4 \times 3 1/2 \times 1/4$	$5 1/2$
8S2	W8 × 21	$6 \times 3 1/2 \times 3/8$	6	2	$3 1/2$	$4 \times 3 1/2 \times 1/4$	$5 1/2$
8S3	W8 × 21	$6 \times 3 1/2 \times 3/8$	8	2	$3 1/2$	$4 \times 3 1/2 \times 1/4$	$5 1/2$
8S4	W8 × 21	$6 \times 3 1/2 \times 3/8$	6	$4 1/2$	$3 1/2$	$4 \times 3 1/2 \times 1/4$	$5 1/2$
8S5	W8 × 21	$6 \times 3 1/2 \times 5/16$	8	$2 1/2$	$5 1/2$	$4 \times 3 1/2 \times 1/4$	$5 1/2$
8S6	W8 × 21	$6 \times 4 \times 5/16$	6	$2 1/2$	$3 1/2$	$4 \times 3 1/2 \times 1/4$	$5 1/2$
8S7	W8 × 21	$6 \times 4 \times 3/8$	6	$2 1/2$	$3 1/2$	$4 \times 3 1/2 \times 1/4$	$5 1/2$
With $7/8$ in bolt diameter							
14S5	W14 × 38	$6 \times 4 \times 3/8$	8	$2 1/2$	$5 1/2$	$4 \times 3 1/2 \times 1/4$	$8 1/2$
14S6	W14 × 38	$6 \times 4 \times 1/2$	8	$2 1/2$	$5 1/2$	$4 \times 3 1/2 \times 1/4$	$8 1/2$
14S8	W14 × 38	$6 \times 4 \times 5/8$	8	$2 1/2$	$5 1/2$	$4 \times 3 1/2 \times 1/4$	$8 1/2$
14S9	W14 × 38	$6 \times 4 \times 1/2$	8	$2 1/2$	$5 1/2$	$4 \times 3 1/2 \times 1/4$	$8 1/2$
8S8	W8 × 21	$6 \times 3 1/2 \times 5/16$	6	2	$3 1/2$	$4 \times 3 1/2 \times 1/4$	$5 1/2$
8S9	W8 × 21	$6 \times 3 1/2 \times 3/8$	6	2	$3 1/2$	$4 \times 3 1/2 \times 1/4$	$5 1/2$
8S10	W8 × 21	$6 \times 3 1/2 \times 1/2$	6	2	$3 1/2$	$4 \times 3 1/2 \times 1/4$	$5 1/2$

1 in = 25.4 mm

rectangular consisting of angle length and gage distance g (Fig. 2b).

Model BM- The mesh pattern of model BM is shown in Fig. 2c. The mesh of the connection model is represented using all major connection components: angle, beam, column and bolt. Column,

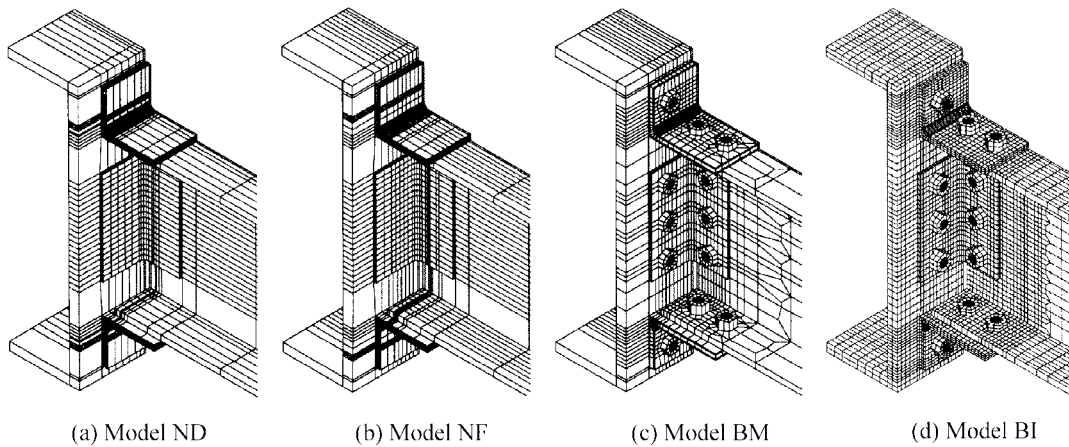


Fig. 2 Mesh patterns of FE models

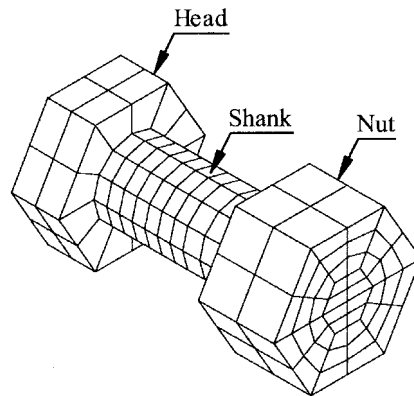


Fig. 3 Mesh pattern of bolt of model BI

beam and angle are completely independent from (i.e. not jointed to) each other and interactions are taken into consideration whenever they come in contact with each other. However, the bolts are assumed not to interact with other components of connection. This model represents the bolt parts, e.g., bolt shank, head, and nut. The bolts in top and seat angles are assumed to behave as two parts: angle-side bolt and flange-side bolt. The angle-side bolt is considered to be a monolithic part of angle whereas the flange-side bolt is assumed to be a part of flange. Similarly, bolts of web angles are also constituted of two parts belonging to angles and beam web or column flange.

Model BI-This model is represented by all major components similar to the model BM and is discretized with fine mesh (Fig. 2d). Bolts are more precisely constructed using eight-node solid elements and are divided to consider the effect of shank, head and nut elements on connection behavior. The bolt hole is made 1.6 mm (1/16 inch) bigger than the bolt diameter, according to the experiments by Azizinamini *et al.* Mesh of a bolt is depicted in Fig. 3. In this model, all components including bolts are completely independent from each other as assemblages in a real connection. Contact interactions are considered between the vertical leg of top or seat angle and column flange, between the horizontal leg of top or seat angle and corresponding beam flange, between web angle's column facing leg and column flange, and between web angle's beam facing leg and beam web. The contact interactions also are considered when bolt and bolt hole elements come into contact with each other. Bolt pretension equal to 0.7 of minimum tensile strength of bolt based on test data is considered for all bolts of the model BI.

3.1 Material properties

Stress-strain relation of steel is represented by using a bilinear constitutive model. Isotropic strain-hardening rule is applied for plastic deformation of steel. ASTM A36 steel was used for the beam, column and angles. The yield stress and ultimate strength for angles are taken from the mean value of coupon test results and similar values are assumed for beam and column. Bolt yield stress and ultimate strength are assumed based on the nominal properties of A325 bolts, since no coupon test results were reported for beam, column and bolt. Effective material properties of connection assemblages are shown in Table 2.

Table 2 Material properties of connection elements used in analysis

Connection components	ASTM designation	Yield stress (MPa)	Ultimate strength (MPa)	Ultimate elongation (%)	Modulus of elasticity (MPa)	Poisson's ratio
Bolt	A325	634.3	930.8	8	2.0×10^5	0.3
With $3/4$ in bolt diameter						
Angle, beam, column	A36	280.3	471.8	20	2.0×10^5	0.3
With $7/8$ in bolt diameter						
Angle, beam, column	A36	272.7	468.5	20	2.0×10^5	0.3

3.2 Boundary conditions and loading

Numerical analyses were performed following the experimental setup and loading method of Azizinamini *et al.* (1985). In these, 1) two beams are symmetrically connected to the stub column flanges, 2) the ends of these beams are simply supported, and 3) the center point of bottom surface of stub column is allowed to move upward so that corresponding forces generated from the prescribed bending moment can be distributed among the connection assemblages. Additionally, rollers are used to correct any movement of the stub column due to slipping and asymmetry. Based on the experimental boundaries, one-quarter model of connection including stub column, beam, top and seat angles, web angle and bolts are used for numerical analysis considering structural symmetry. Fig. 4 demonstrates the boundary conditions applied to the FE models. To enforce connection symmetry, all nodes of the stub column in the middle of the plane 3-1 have been restrained displacement in the direction of 2. In the middle section of beam parallel to the 2-3 plane, all nodes are constrained in the direction of 1 (Fig. 4). To produce only vertical reaction forces, the beam end support is assumed as pin.

The analysis was carried out with only one incremental loading step for all models except for

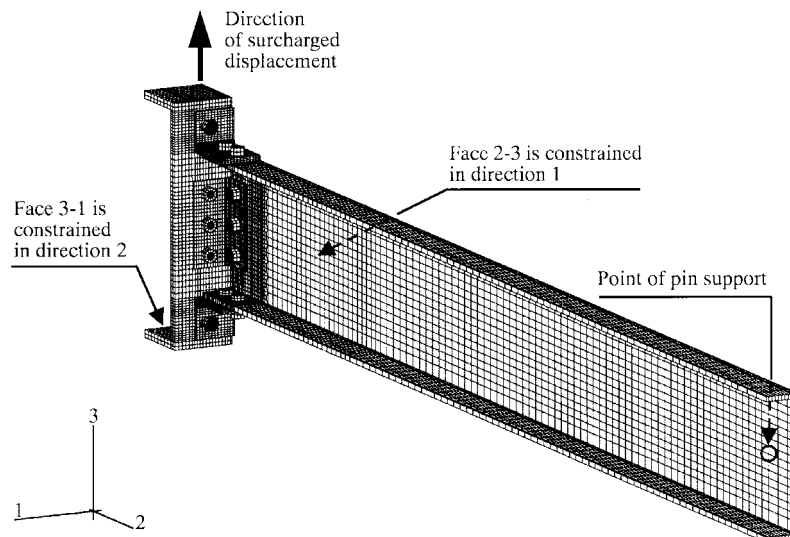


Fig. 4 Boundary conditions of FE model

model BI. Connection moment is surcharged by applying upward displacement to the middle section of plane 3-1 of the stub column. Model BI is analyzed using three loading steps. In the first step, a prescribed force of 0.7 of minimum tensile strength of bolt is applied to the pretension node of a pre-defined section of bolt shank. As a result, the length of bolt shank at the pretension section changes by the amount necessary to carry the prescribed load. In the second step, the prescribed bolt load is replaced by changing the length of pretension section back to the initial length. In the third step, bending moment is introduced on beam-to-column connection by employing vertical displacement of the middle section of plane 3-1 of the stub column. Automatic load increment scheme is preferred because ABAQUS tool selects increment size based on computational efficiency.

3.3 Contact modeling

To simulate accurately the connection behavior, small sliding contact pair definition is applied between two interacting surfaces, one of which is defined as master surface and the other as slave surface. Master surfaces of contact pair options represent the surfaces of column and beam flanges, beam web and bolts, whereas the surfaces interfacing master surfaces are defined as slave surfaces. Coulomb's frictional coefficient is assumed as 0.1.

3.4 Verification and model selection

Verification of the analytical results of the four models mentioned above is made by comparison with the test results of Azizinamini *et al.* (1985). A representative example of test specimen 14S2 is shown in Fig. 5. The values of initial connection stiffness and ultimate moment capacity corresponding to this figure are listed in Table 3. The FE analysis results are almost identical to the experimental curve in the linear elastic range. However, a discrepancy exists between the FE analysis prediction and the experimental results in the plastic range. It is obvious that, among four models, model BI most closely predicts the moment-rotation behavior of the connection. For ultimate moment capacity and initial connection stiffness, its respective deviations from the experimental

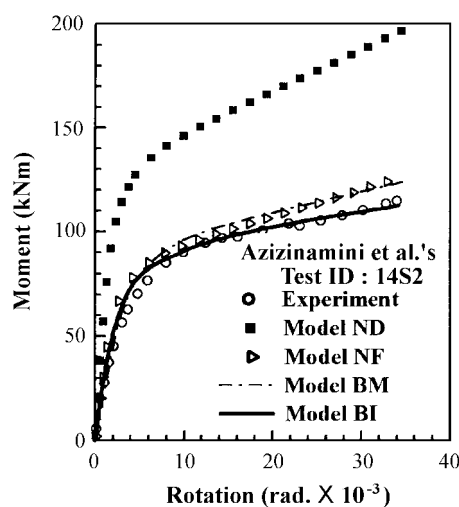


Fig. 5 Comparison among models

Table 3 Pertinent data of Fig. 5 (Test ID: 14S2)

FE Model or Experiment	Initial connection stiffness		Ultimate moment capacity	
	Result (kNm/rad.)	Error (%)	Result (kNm)	Error (%)
ND	69,619	+31.8	195.6	+70.5
NF	38,612	-26.9	125.3	+9.2
BM	40,025	-24.3	123.0	+7.2
BI	41,388	-21.7	112.5	-1.9
Test	52,839	-	114.7	-

results are -1.9% and -21.7% . The mesh arrangements of models ND and NF are simple but do not contain all essential characteristics and components of connection. In contrast, models BM and BI represent the real situation of connection assemblages. Fig. 5 and Table 3 show that models NF, BM, and BI are able to produce an acceptable accuracy. Model BI best represents the real interactions among the connection components. In light of this, model BI was chosen for the present study.

4. Three-parameter power model for connections with angles

Based on Richard and Abbott's power function (1975), Kishi and Chen in 1990 proposed a three-parameter power model disregarding the strain-hardening effect. The model is used here to compare the nonlinear $M-\theta_r$ curve of top- and seat-angle with double web-angle connections with corresponding curves, spread of yield stresses and deformations for FE analysis calculated and measured values in experiment. The power model containing three parameters: initial connection stiffness R_{ki} , ultimate moment capacity M_u , and shape parameter n , has the following form:

$$M = \frac{R_{ki} \theta_r}{[1 + (\theta_r / \theta_0)^n]^{1/n}} \quad (1)$$

where M and θ_r are moment and relative rotation in connection, respectively; and θ_0 is a reference plastic rotation, $\theta_0 = M_u / R_{ki}$. Fig. 6 shows the general shapes of $M-\theta_r$ curves of Eq. (1) with different values of shape parameter n . The initial connection stiffness, R_{ki} is determined from the following equation:

$$R_{ki} = \frac{3EI_t}{1 + \frac{0.78t_t^2}{g_1^2}} \frac{d_1^2}{g_1^3} \quad (2)$$

where EI_t is the bending stiffness of top angle's vertical leg; $g_1 = g - D/2 - t_t/2$; $D = w$ for bolted connections; or, $D = d_b$ for riveted connections; d_b is the fastener's diameter, $d_1 = h_b + t_t/2 + t_s/2$; h_b is the beam height; t_t and t_s are the thicknesses of top and seat angles, respectively. The shape parameter n is determined by using a subroutine of least mean square technique for the differences between the predicted moments and those of the experimental results that developed by Chen and Kishi (1989).

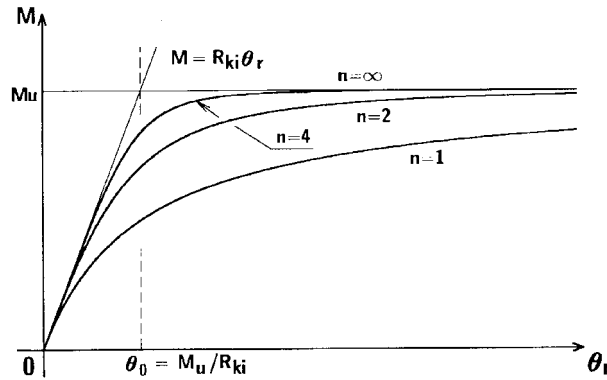


Fig. 6 Three-parameter power model

5. Analysis results and comparisons

5.1 Moment-rotation behavior

To justify the validity of model BI, the eighteen bolted connections of Azizinamini *et al.* (1985) were analyzed. The geometrical measurements of connections are shown in Table 1. The $M-\theta_r$ curves obtained from FE analysis together with Kishi-Chen power model (1990) and experimental data (1985) are shown in Fig. 7. The connection moment M is evaluated by multiplying reaction force and minimum distance between the supporting point of beam end and the instantaneous center of rotation. Relative rotation of the connection evaluated from the results of FE analysis is estimated using the equation: $\theta_r = (\delta_t - \delta_b) / h_b$, where δ_t and δ_b are the horizontal displacements at the upper and lower edges of beam flanges, respectively. Analytical values of initial connection stiffness and ultimate moment capacity are listed in Table 4. The figures show that these three results agree closely. From Table 4 and Fig. 7, it is evident that the discrepancies on ultimate moment capacity between FE analysis and experimental results range from -15.4% to $+6.1\%$, and the power model prediction of moment-rotation characteristics of top- and seat-angle with double web-angle connections agrees fairly closely with test results except a few cases.

5.2 Deformation and stress distribution of connection

Here, taking the connection model 14S2 as a connection example, deformation and stress distribution of top- and seat-angle with double web-angle connection are discussed. Fig. 8 shows the deformation configuration of connection at the ultimate state. This figure indicates that severe deformation occurs in the vertical leg of top angle in the vicinity of bolt hole and that the maximum horizontal displacement in the top angle occurs at the heel. The connection rotates around the instantaneous center near the toe of fillet of horizontal leg of seat angle. This indicates that the rotation of connection may be approximated by dividing the maximum horizontal displacement of the heel of top angle by the distance between the heels of the top and seat angles, as discussed earlier.

The corresponding Mises stress distribution at the ultimate state for the connection 14S2 is shown in Fig. 9. The color contours in the plots represent the magnitude of stress. The figure reveals that comparatively greater stress is generated mainly in the top angle, which is in tension. It is also

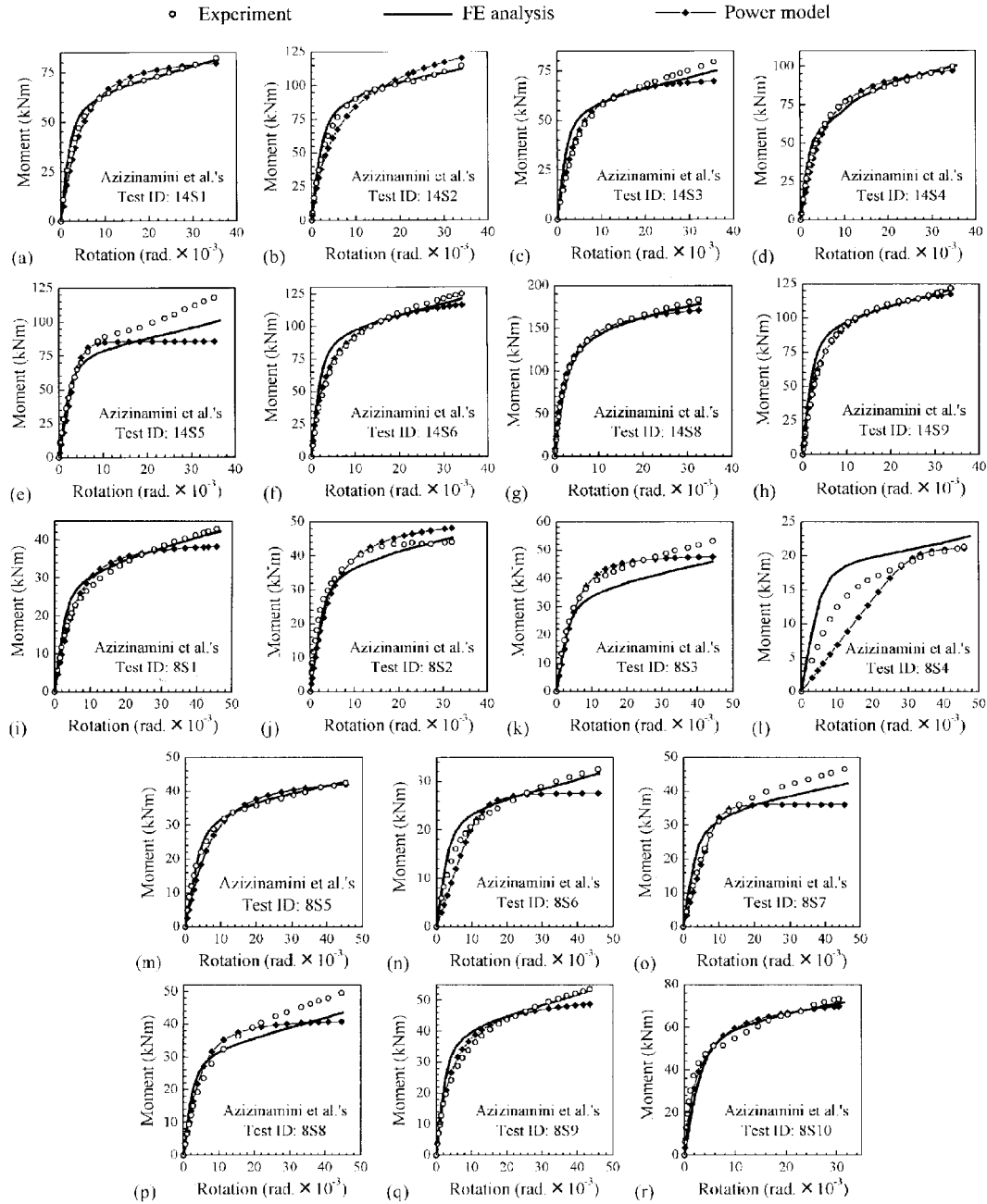


Fig. 7 Performance of FE analysis and power model

shows that smaller stress develops in beam and column which is under the elastic range, excepting the stress concentration area near the bolt holes in beam web and column flange. Stress contour plots for tension bolt and each angle are depicted in Figs. 10 and 11. These figures show the results for two stages of loading: in the state after introduction of pretension force (Figs. 10a and 11a), and at the ultimate state of connection (Figs. 10b and 11b-e). The results on stress distributions of σ_{22} in

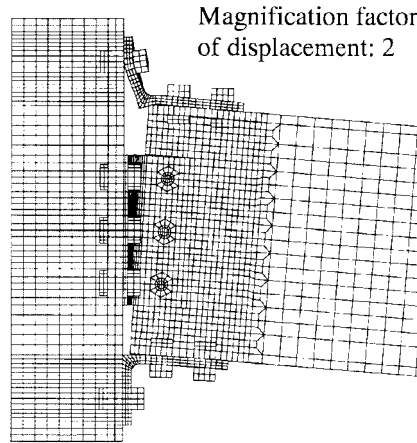


Fig. 8 Deformation configuration of connection 14S2 at ultimate state

Table 4 Predicted initial connection stiffness and ultimate moment capacity with test result

Test ID	Initial connection stiffness, R_{ki} (kNm/radian)			Ultimate moment capacity, M_u (kNm)			Shape parameter, n of power model
	Experiment	FE analysis	Power model	Experiment	FE analysis	Power model	
14S1	31,798	22,582	16,362	82.2	81.5	83.0	1.499
14S2	52,839	41,388	39,855	114.7	112.5	170.7	0.678
14S3	14,306	20,709	15,730	79.5	75.1	72.3	1.506
14S4	25,165	26,969	21,165	99.4	99.8	105.0	1.240
14S5	61,755	24,530	19,312	117.9	99.8	85.6	4.587
14S6	28,928	35,608	47,200	125.1	120.8	134.5	0.865
14S8	66,049	46,356	98,446	183.6	178.4	187.3	0.904
14S9	27,764	35,608	47,200	121.6	120.8	134.5	0.880
8S1	8,353	7,866	6,165	42.9	42.1	39.4	1.657
8S2	27,199	9,901	11,076	44.1	45.3	51.6	1.307
8S3	12,385	8,184	8,092	53.2	45.9	48.3	1.980
8S4	1,878	3,115	7,734	21.3	22.6	21.2	8.851
8S5	10,317	6,603	5,544	42.5	42.7	43.9	1.599
8S6	6,783	5,550	2,497	32.5	31.6	27.6	4.255
8S7	4,951	7,026	4,256	46.5	42.1	36.1	5.320
8S8	7,026	8,217	7,736	49.5	43.4	41.5	1.747
8S9	13,176	10,738	13,956	53.6	53.1	53.4	1.018
8S10	61,472	14,735	36,714	73.4	71.6	77.2	0.921

tension bolt (Fig. 10a) and Mises stress in top angle (Fig. 11a) confirm that 1) tensile stress distributes uniformly in the whole bolt shank except the area near bolt head and nut, 2) slightly greater stress develops through the whole section of those regions, and 3) the contact pressure on top angle's vertical leg under the nut caused by tightening force is distributed almost uniformly. Fig. 10b shows stress distribution of σ_{22} in tension bolt at the ultimate state of connection. The figure reveals that 1) bolt shank is loaded combining with two axial forces (pretension force and bending tension force due to connection moment) and bending moment that develops because both

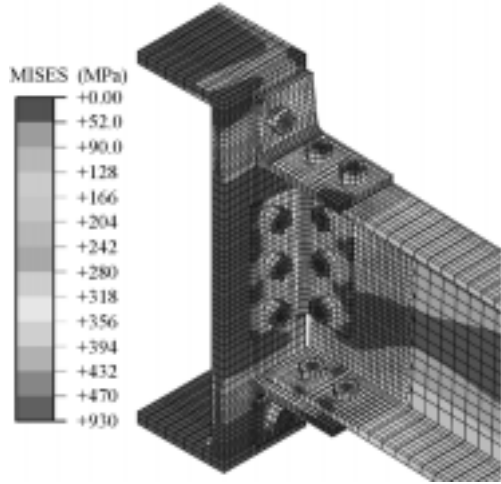


Fig. 9 Von Mises stress contour plot of connection 14S2 at ultimate state

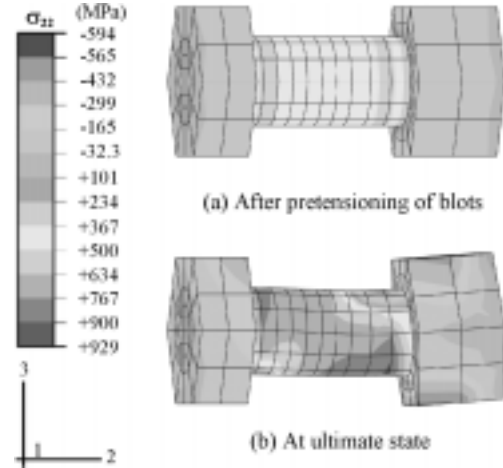


Fig. 10 σ_{22} stress contour plot of tension bolt of connection 14S2

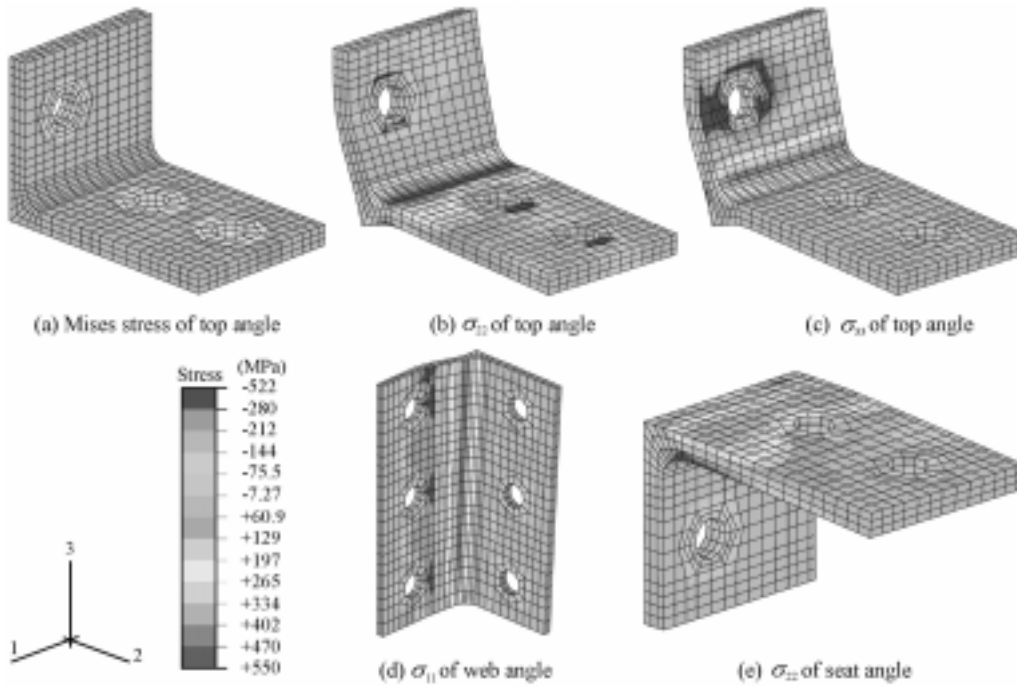


Fig. 11 Deformation and stress contour plot of angles of connection 14S2: (a) just after pretensioning of bolts; (b)-(e) at ultimate state ($M_{ir}=112.5$ kNm)

tensile and compressive stresses are occurred in the bolt shank; 2) These maximum stresses are both greater than that of each yielding limit. The bending moment may be introduced by prying force acting near the upper edge of vertical leg of top angle.

The stress distributions of each angle (Figs 11b-e) indicate that, at first, the toe of the fillet of top

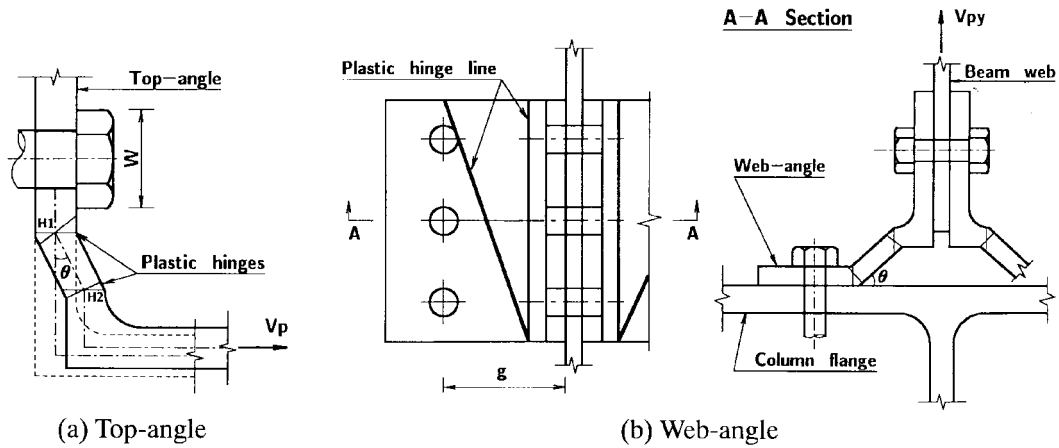


Fig. 12 Failure mechanisms at the ultimate state

angle's horizontal leg yields, and then yielding is followed by that of the toe of the fillet of top angle's vertical leg. The area along the compressive stress lines near bolt holes of top and web angles finally falls at the yield stress state. The vertical leg of seat angle, which is under compressive loading, is less stressed since its whole surface contacting the column flange is pushed against the flange in the connection arrangement (Fig. 11e). However, the stress of lower fiber at the toe of fillet of seat angle's horizontal leg increases to the ultimate level. Web angles act as cantilever beam similar to the top and seat angles because plastic hinge is formed along the bolt line of leg connected to the column flange. It is observed and recognized that web angles transfer not only beam shear force but also connection moment to the column. Azizinamini *et al.* mentioned a similar history of connection angle deformation at different stages of loading in their test (1985). They reported that the plastic hinge spreads subsequently through the length of the top angle, at the lower portion of bolt hole area and at the toe of fillet of top angle's vertical leg.

The plastic hinge lines at the ultimate state assumed by power model are shown in Fig. 12. It is evident from Figs. 11c-d and Fig. 12 that the maximum stress concentrations predicted by FE analysis at top and web angles are at the exact same places as those assumed by power model for the calculation of ultimate moment capacity of connection.

6. Remarks and conclusions

This study is focused primarily on finding the most suitable FE technique to predict moment-rotation behavior of top- and seat-angle with double web-angle connections under monotonic loading. Verifications of the FE technique and a moment-rotation power model also were made. A comparative study of FE methodology, power model prediction, and experimental results reveal the following:

- A) FE analysis and experimental evidence verify the failure mechanism assumed by power model. Spread of yield stresses and deformation at the ultimate state of connection obtained from FE analysis and experiment show close agreement.

- B) Moment-rotation curves predicted by the three methods agree closely.

The followings can be concluded:

1. The three-parameter power model can be used as an efficient and reasonably accurate prediction model.
2. FE technique can also be a viable approach in establishing a semi-rigid frame analysis method, particularly for connections whose analytical formulations are not available. However, this procedure inherently tends to require much more computing time than its analytical counterpart.
3. The capability of FE technique to simulate real connection behavior under monotonic loading indicates the potential of the technique for modeling of cyclic loading.

References

- ABAQUS/Standard (1998), *User's Manual*, **I-III**, Version 5.8, Hibbitt Karlsson & Sorensen, Inc.
- American Institute of Steel Construction (1989), *Manual of Steel Construction, Allowable Stress Design Specification*, AISC, Chicago.
- American Institute of Steel Construction (1994), *Manual of Steel Construction, Load and Resistance Factored Design*, AISC, Chicago, **I & II(2)**.
- Azizinzmini, A., Bradburn, J.H., and Radzimirski, J.B. (1985), "Static and cyclic behavior of semi-rigid steel beam-column connections," *Structural Research Studies*, Department of Civil Engineering, University of South Carolina, Columbia, S.C., March.
- Chen, W.F., and Kishi, N. (1989), "Semi-rigid steel beam-to-column connections: Data base and modeling," *J. Struct. Eng.*, ASCE, **115**(1), 105-119.
- Colson, A., and Louveau, J.M. (1983), "Connections incidence on the inelastic behavior of steel structures," *Euromech Colloquium*, **174**, October.
- Frye, M.J., and Morris, G.A. (1975), "Analysis of flexibly connected steel frames," *Canadian J. Civil Eng.*, **2**(3), 280-291.
- Jones, S.W., Kirby, P.A., and Nethercot, D.A. (1980), "Effect of semi-rigid connections on steel column strength," *J. Constr. Steel Res.*, **1**(1), 38-46.
- Jones, S.W., Kirby, P.A., and Nethercot, D.A. (1981), "Modeling of semi-rigid connection behavior and its influence on steel column behavior," *Joints in Structural Steelwork*, J.H. Howlett, W.M. Jenkins and R. Stainsby, eds, Pentech Press, London, 5.73-5.78.
- Kishi, N., and Chen, W.F. (1986), "Data base of steel beam-to-column connections," *Struct. Eng.*, Report No. CE-STR-86-26, School of Civil Engineering, Purdue University, West Lafayette, IN.
- Kishi, N., and Chen, W.F. (1990), "Moment-rotation relations of semi-rigid connections with angles," *J. Struct. Eng.*, ASCE, **116**(7), 1813-1834.
- Lightfoot, E., and LeMessurier, A.P. (1974), "Elastic analysis of frameworks with elastic connections," *J. Struct. Div.*, ASCE, **100**(6), 1297-1309.
- Lui, E.M., and Chen, W.F. (1983), "Strength of H-columns with small end restraints," *J. Institution of Struct. Eng. (London)*, **61B**(1), 17-26.
- Lui, E.M., and Chen, W.F. (1986), "Analysis and behavior of flexibly jointed frames," *Eng. Struct.*, Butterworth, U.K., **8**, 107-118.
- Monforton, A.R., and Wu, T.S. (1963), "Matrix analysis of semi-rigidly connected frames," *J. Struct. Div.*, ASCE, **87**(6), 13-42.
- Rathbun, J.C. (1936), "Elastic properties of riveted connections," *Trans. ASCE*, Paper No.1933, **101**, 524-563.
- Richard, R.M., and Abbott, B.J. (1975), "Versatile elastic-plastic stress-strain formula," *J. Eng. Mech. Div.*, ASCE, **101**(4), 511-515.
- Tarpy, T.S., and Cardinal, J.W. (1981), "Behavior of semi-rigid beam-to-column end plate connections," *Joints in Struct. Steelwork*, J.H. Howlett *et al.*, eds, Pentech Press, London, 2.3-2.25.
- Wu, F.H., and Chen, W.F. (1990), "A design model for semi-rigid connection," *Eng. Struct.*, **12**(2), 88-97.
- Yee, Y.L., and Melchers, R.E. (1986), "Moment-rotation curves for bolted connections," *J. Struct. Eng.*, AISC, **112**(3), 615-635.